Geofísica Internacional (2007), Vol. 46, Num. 2, pp. 141-147

Tidal Current Components in the Southern Bay of Campeche, Gulf of Mexico

David A. Salas-de-León[1], María A. Monreal-Gómez[1], David Salas-Monreal[2], Gilberto Expósito-Díaz[1], Mayra L. Riverón-Enzastiga[1] and Felipe Vázquez-Gutiérrez[1]

[1] *Instituto de Ciencias del Mar y Limnología, Universidad Nacional Autónoma de México, Mexico City, Mexico*

[2] *Centro de Ecología y Pesquerías, Universidad Veracruzana, Veracruz Mexico*

Received: March 17, 2006 ; accepted: May 17, 2007

Resumen

Datos sobre la magnitud y dirección de las corrientes fueron obtenidos en la Bahía de Campeche, al sur del Golfo de México, de marzo a mayo de 1997, para obtener las principales componentes de marea en la región. Las elipses y fases de las diferentes componentes de marea fueron obtenidas mediante un ajuste por mínimos cuadrados acoplado con una modulación nodal a partir de las series horarias de corrientes por marea. Los constituyentes P_1 y K_2 se infirieron a partir de los constituyentes K_1 y S_2, respectivamente. Los resultados muestran la dominancia del armónico K_1 en la plataforma continental al sur de la Bahía de Campeche, una región de mareas mixtas con dominancia semidiurna en la zona del umbral de Cayo Arcas y una región de transición entre Cayo Arcas y las estaciones al oeste en la zona de estudio. Las diferencias en las amplitudes de las corrientes de marea en la vertical fueron despreciables, mientras que las diferencias en las fases muestran un retraso significativo entre la superficie y el fondo. El sentido de rotación de las elipses de marea en Cayo Arcas es negativo, mientras que en las otras estaciones fue positivo. Cayo Arcas tiene una fuerte influencia en las corrientes de marea ya que su fase y sentido de rotación varían.

Palabras clave: Corrientes de marea, armónicos de marea, Bahía de Campeche, Golfo de México

Abstract

Current velocity data in the Southern Bay of Campeche, Gulf of Mexico, were obtained from March 1997 to May 1997, in order to compute tidal ellipses and phase lags in the region. Tidal ellipses and phase lags were calculated via a least squares fit method coupled with nodal modulation from the hourly time series. Constituents P_1 and K_2 were inferred from K_1 and S_2, respectively. The K_1 component is dominant in the southern shelf of the Bay of Campeche, a region of mixed tides with semidiurnal dominance at the Arcas Kay sill, and a transition region between Arcas Kay and the southern-western stations. Vertical differences in tidal current amplitudes were negligible. There was a significant phase lag from surface to bottom. The sense of rotation for the tidal ellipses near Arcas Kay was negative, while at other stations it was positive. Arcas Kay has a strong influence on tidal currents because of vertical phase and sense of rotation variation with depth.

Key words: Tidal currents, tidal harmonics, Bay of Campeche, Gulf of Mexico.

Introduction

Hydrodynamics of coastal ocean waters features a variety of processes, including the tides. The Bay of Campeche (Figure 1) is a region of major economical activities such as petroleum production and fisheries.

However, the coastal circulation in the Bay of Campeche is not fully understood.

Typical water depths are less than 200 m. Beyond the shelf edge, depths increase rapidly to values over 1000 m, and reach more than 3000 m at the centre of the bay. The tides in the region are diurnal (Grace, 1932) with an amphidromic point for M_2 (Figure 2) off the western Yucatan peninsula (Salas-de-León, 1986; Salas-de-León and Monreal-Gómez, 1997). Near the port of Campeche tides are mixed, with diurnal dominance (Salas-de-León, 1986). In the southwestern part of the bay, tides are diurnal as shown by the form number (Salas-de-León and Monreal-Gómez, 1998).

Currents in the Bay of Campeche follow the bathymetry. The M_2 tidal component from the southern Gulf of Mexico enters by the Yucatan Channel turns westward at the amphidromic point near Progreso, and flows toward the Bay of Campeche by Arcas Key (Figure 2). Low amplitudes were observed near Coatzacoalcos while, the highest tides were found at Arcas Key and near Isla Del Carmen. The obtained magnitude and

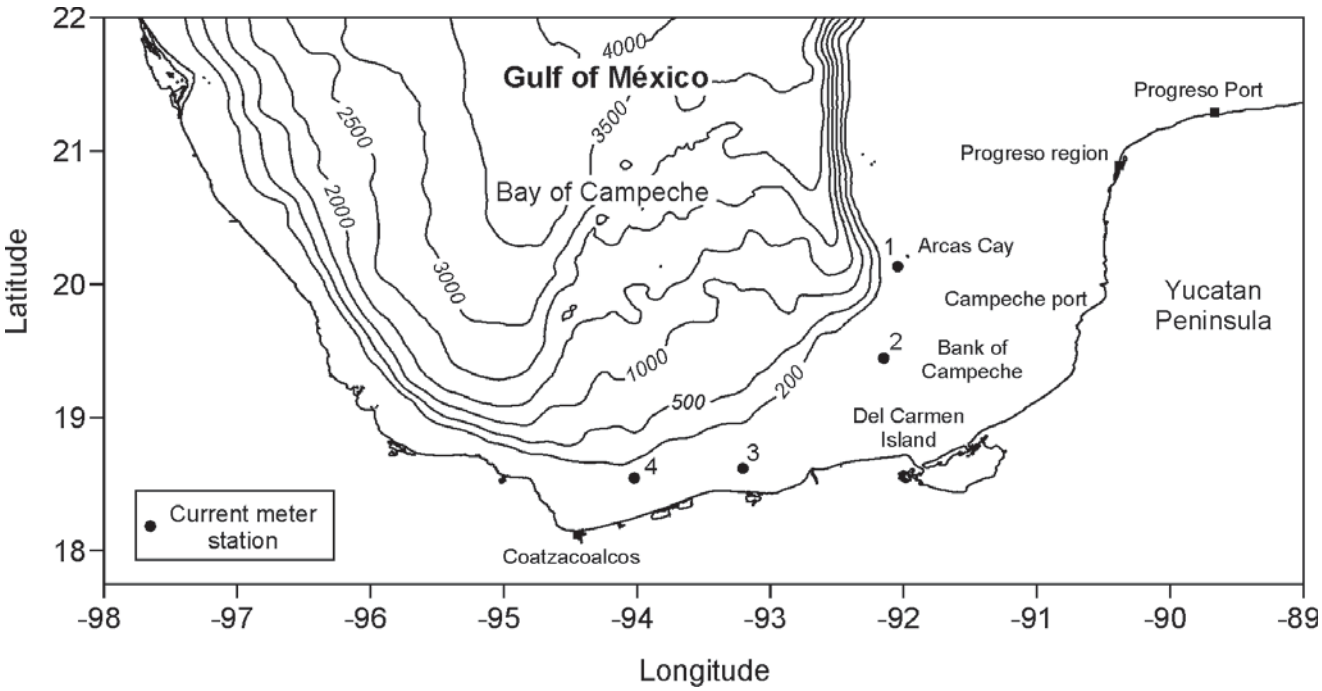

Fig. 1. Bay of Campeche, with mooring positions of current-meters. Depth contours in meters.

direction of tidal currents for the points corresponding to the anchorages (Salas-de-León, 1986), were as follows: C1, 0.41 cm s^{-1} and 101°; C2, 0.32 cm s^{-1} and 122°; C3, 0.09 cm s^{-1} and 125°; and C4, 0.04 cm s^{-1} and 147°. There is no further information on tidal currents in the Bay of Campeche.

In this study we present a tidal current analysis for the region. Results on sub-inertial frequencies will be published separately. Our data were collected over a three month period, and include coastal circulation relative to tides, wind data, atmospheric pressure and non-local forcing. Results from this study are expected to improve coastal management procedures for the region and provide information for emergency situations in case of oil spills.

Methods

A total of ten RCM4 and RCM7 Aanderaa current meters were deployed from March 1997 to May 1997 at four mooring sites (Figure 1 and Table 1). The current meters record velocity, temperature, conductivity, and water pressure; temperature, conductivity, and water pressure data were not used in this analysis. The positions of the moored current meters were obtained from the GPS navigation system aboard the R/V "Justo Sierra" of the Universidad Nacional Autónoma de México (Table 1). Calibration of the instruments and data quality analysis were performed by V. G. Koutitonsky at the University of Québec, in Rimouski, Canada.

Table 1

Location, geographical position and depth of current meter stations

Station number	Latitude (N)	Longitude (W)	Total depth (m)
1	20° 08.035'	92° 02.601'	77.0
2	19° 26.762'	92° 08.957'	51.3
3	18° 37.199'	93° 12.337'	28.0
4	18° 32.868'	94° 01.216'	75.5

Two or three current meters were moored at different depths (Table 2). Sampling interval was 20 minutes. Hourly time series were filtered with a Godin-type low-pass filter $A^2_4A_5$ (Emery and Thompson, 1998). Frequencies higher than 1.38×10^{-4} s^{-1}, equivalent to a 2 h period, were removed. The filter does not produce phase lags (Salas-Monreal, 2006).

Tidal ellipse parameters and Greenwich phase lags were calculated via a least squares fit coupled with nodal modulations. This analysis was carried out only for constituents that could be resolved over the length of the record (e.g., Godin, 1972; Godin, 1976; Foreman, 1996). Constituent P_1 and K_2 were inferred from K_1 and S_2, respectively.

Table 2

Instrument type, stations, sampling depth, start and end recording times. The year was 1997, and the time is in GMT (- 6 h). C, current meter, station numbers are as in Figure 1. S, M, and B is surface, mid water and bottom.

Instrument on the mooring line (identification name)	Sampling Depth (m)	Start GMT Time	End GMT Time
RCM7 (C1S)	36.5	22:40/06/03	11:20/22/05
RCM4 (C1B)	70.5	22:40/06/03	15:20/27/04
RCM7 (C2S)	23.0	16:20/06/03	19:00/21/05
RCM4 – S (C2M)	34.5	16:20/06/03	19:00/21/05
RCM4 (C2B)	44.5	16:20/06/03	19:00/21/05
RCM4 – S (C3S)	16.0	17:40/03/03	19:00/12/06
RCM4 – S (C3B)	23.5	17:40/03/03	19:00/12/06
RCM4 – S (C4S)	17.3	17:40/02/03	12:00/20/05
RCM4 – S (C4M)	47.5	17:40/02/03	12:00/20/05
RCM4 (C4B)	66.0	17:40/02/03	12:00/20/05

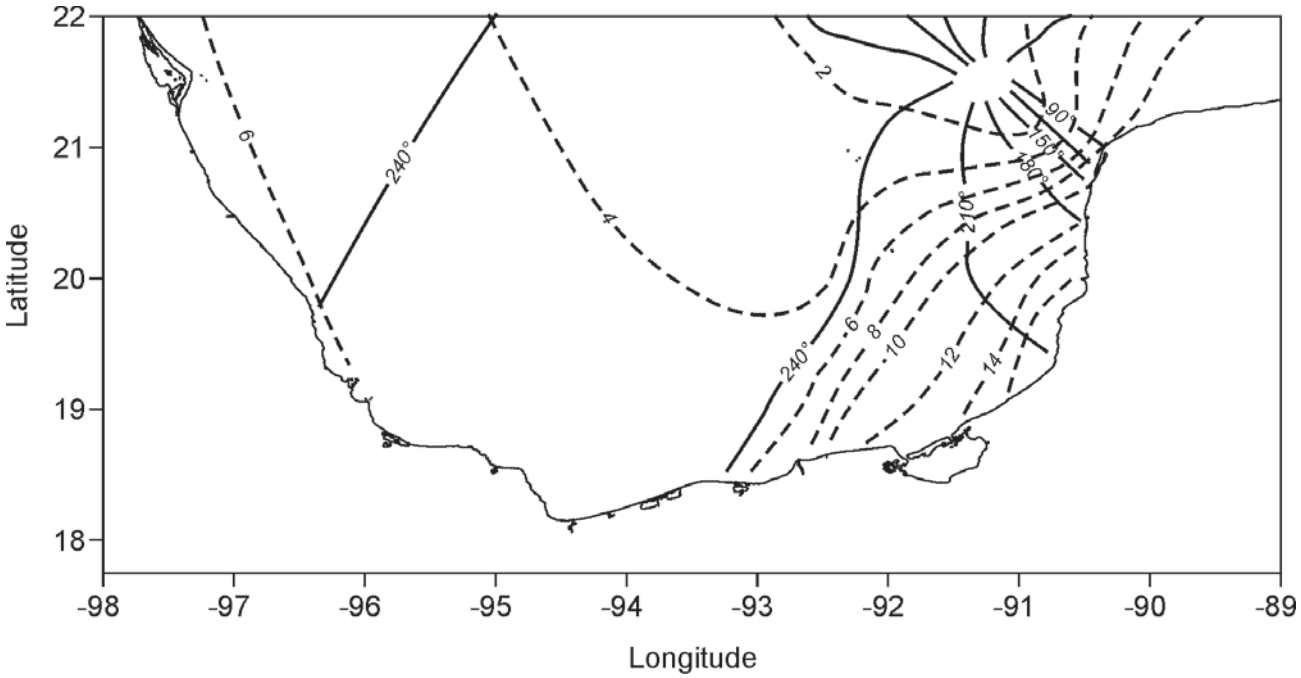

Fig. 2. M_2 cotidal lines. Amplitude (dashed, in cm) and phase (solid, GMT, in degrees). After Salas-de-León and Monreal-Gómez (1997).

Results and discussion

Main tidal current constituents were calculated for each station and depth (Tables 3 to 6). Major ($a^+ + a^-$) and minor ($a^+ - a^-$) ellipses, angles of inclination (θ) with positive *x* axis (Figure 3), phases (*g*) relative to Greenwich and constant phase angles (g^+ and g^-) for each constituent were reported as in Godin (1972). Unfortunately, current meter C2B proved to be unusable.

Tidal constituent K_1 was dominant for nearly all surface tidal currents, down to mid water depths. However, at station 4 the main constituent of the surface tidal current was OO_1. Near the bottom, the dominant constituent varied from one position to another. At station 1 the dominant component was O_2, while at station 3 it was $2Q_1$ and at station 4 the Q_1 constituent.

The period of oscillation of tidal currents was approximately 24 h. Thus diurnal tidal components were

Table 3

Tidal current analysis results for current meter C1. Results are in tidal ellipse (cm s^{-1}) form. Phases are referred to GMT

	C1S						*C1B*					
NAME	$a^+ + a^-$	$a^+ - a^-$	θ	g	g^+	g^-	$a^+ + a^-$	$a^+ - a^-$	θ	g	g^+	g^-
$2Q_1$	0.589	0.091	94.5	122.5	28.0	217.0	0.471	0.230	127.1	254.9	127.8	22.0
Q_1	1.242	0.952	129.8	200.9	71.1	330.7	1.625	1.161	153.2	251.0	97.8	44.2
O_1	2.730	2.542	177.4	347.4	170.0	164.8	2.780	1.274	138.7	283.0	144.3	61.7
NO_1	1.567	0.612	68.9	296.9	228.0	5.7	1.047	0.581	148.2	3.3	215.1	151.5
P_1	1.955	1.646	78.7	317.3	238.6	36.0	1.861	1.467	105.1	297.3	192.1	42.4
K_1	6.558	4.991	80.8	315.0	234.1	35.8	6.334	4.339	107.3	294.9	187.6	42.2
J_1	1.340	0.582	121.6	319.2	197.6	80.9	1.306	-0.207	86.2	61.8	335.5	148.0
OO_1	0.893	0.415	3.3	56.9	53.6	60.2	1.835	-0.010	179.3	295.0	115.7	114.2
ε_2	0.574	0.006	95.7	114.9	19.1	210.6	0.227	-0.028	104.0	254.1	150.0	358.1
μ_2	0.293	-0.060	110.6	102.4	351.8	213.0	0.640	0.267	102.4	209.1	106.7	311.6
N_2	1.195	0.365	88.1	146.8	58.7	234.9	1.062	0.279	101.0	91.1	350.1	192.1
M_2	5.171	1.826	90.6	173.5	82.9	264.0	4.061	1.368	100.2	124.5	24.2	224.7
L_2	0.346	-0.023	48.4	63.8	15.4	112.3	0.942	0.117	131.9	45.9	274.1	177.8
S_2	1.176	0.249	82.8	193.0	110.1	275.8	0.873	0.343	87.0	95.7	8.7	182.7
K_2	0.235	0.038	61.8	186.8	124.9	248.6	0.173	0.060	66.0	89.5	23.5	155.5
η_2	0.201	0.122	34.0	153.6	119.5	187.6	0.708	0.222	132.0	300.1	168.1	72.1
M_3	0.431	0.266	124.2	139.4	15.2	263.7	0.225	0.012	26.7	224.6	198.0	251.3
M_4	0.066	0.036	128.2	163.2	35.0	291.4	0.099	0.063	133.3	157.8	24.5	291.1
S_4	0.123	-0.046	138.8	182.4	43.6	321.3	0.139	-0.040	66.2	242.4	176.3	308.6

Table 4

Tidal current analysis results for current meter C2. Results are in tidal ellipse (cm s^{-1}) form. Phases are referred to GMT

	C2S						*C2M*					
NAME	$a^+ + a^-$	$a^+ - a^-$	θ	g	g^+	g^-	$a^+ + a^-$	$a^+ - a^-$	θ	g	g^+	g^-
$2Q_1$	1.273	0.579	87.9	135.6	47.8	223.5	1.615	0.724	154.3	191.2	36.9	345.5
Q_1	1.786	0.792	93.4	235.6	142.2	329.0	1.370	0.944	160.3	145.3	345.0	305.6
O_1	2.328	1.242	123.9	258.3	134.3	22.2	1.263	0.819	157.7	316.9	159.3	114.6
NO_1	1.345	0.475	47.1	273.8	226.7	320.8	0.778	-0.263	164.1	324.4	160.4	128.5
P_1	1.287	0.846	105.2	259.9	154.7	5.1	1.317	1.086	89.9	338.3	248.4	68.2
K_1	4.536	2.305	107.4	257.6	150.2	4.9	4.437	3.268	92.1	336.0	243.9	68.0
J_1	0.876	0.284	74.6	353.3	278.7	67.8	1.318	0.329	142.2	59.9	277.7	202.1
OO_1	0.593	-0.014	20.4	341.4	321.0	1.8	0.941	0.377	122.4	212.0	89.6	334.4
ε_2	0.575	0.369	59.0	304.8	245.8	3.8	0.291	0.194	20.3	16.8	356.5	37.1
μ_2	0.522	0.338	54.5	324.0	269.5	18.5	0.245	-0.056	164.8	135.5	330.7	300.4
N_2	0.939	0.656	121.5	19.4	258.0	140.9	0.720	0.302	132.8	138.2	5.4	271.0
M_2	4.101	0.716	112.9	40.2	287.3	153.0	2.429	0.506	104.8	162.4	57.7	267.2
L_2	0.471	-0.202	88.7	64.5	335.8	153.1	0.355	-0.186	79.5	83.9	4.4	163.4
S_2	0.979	-0.101	115.2	55.0	299.8	170.3	0.926	0.108	119.8	157.5	37.7	277.4
K_2	0.199	-0.031	94.2	48.8	314.6	143.1	0.186	0.012	98.8	151.3	52.5	250.2
η_2	0.605	0.295	158.2	67.1	268.9	225.2	0.703	0.286	176.4	240.9	64.5	57.2
M_3	0.203	0.074	75.7	321.5	245.8	37.3	0.239	-0.015	62.4	120.3	57.9	182.7
M_4	0.120	0.004	117.0	320.9	203.9	78.0	0.177	0.096	178.5	352.4	173.9	170.9
S_4	0.151	0.086	18.0	14.1	356.1	32.1	0.118	0.061	102.8	201.1	98.4	303.9

Table 5

Tidal current analysis results for current meter C3. Results are in tidal ellipse (cm s^{-1}) form. Phases are referred to GMT

	C3S						*C3B*					
NAME	$a^+ + a^-$	$a^+ - a^-$	θ	g	g^+	g^-	$a^+ + a^-$	$a^+ - a^-$	θ	g	g^+	g^-
$2Q_1$	1.232	0.834	127.9	149.6	21.7	277.6	1.35	0.609	111.4	136	24.6	247.5
Q_1	1.760	1.376	162.6	94.2	291.7	256.8	1.531	0.977	21	283.2	262.2	304.2
O_1	1.802	1.202	6.4	195.7	189.3	202.1	0.781	0.515	150	349.3	199.3	139.3
NO_1	1.009	0.491	79.1	28.8	309.7	107.9	0.432	0.166	87.1	103.4	16.3	190.5
P_1	1.274	0.946	148.4	283.8	135.4	72.2	0.907	0.652	152.4	279	126.6	71.4
K_1	4.391	2.728	150.5	281.5	130.9	72.0	3.144	1.854	154.5	276.6	122.1	71.2
J_1	1.797	0.210	166.5	291	124.6	97.5	1.216	0.473	159.8	270.2	110.4	70
OO_1	1.679	1.266	119.2	94.4	335.2	213.5	0.889	0.587	58.4	356.3	297.9	54.7
ε_2	0.520	0.181	69.1	13.6	304.5	82.7	0.672	0.383	37	18.4	341.4	55.4
μ_2	0.443	0.044	62.6	264.1	201.5	326.7	0.345	-0.237	129.5	154.5	24.9	284
N_2	0.687	0.363	161.0	316.5	155.5	117.5	0.634	0.453	134	311.7	177.7	85.7
M_2	0.958	0.105	146.0	21.0	235.1	167.0	0.929	0.037	127.5	340.9	213.4	108.4
L_2	0.968	0.322	58.0	303.4	245.4	1.4	0.236	0.124	64.8	309.8	245	14.7
S_2	0.784	0.252	22.0	211.5	189.5	233.5	0.466	0.344	179.9	34.6	214.7	214.5
K_2	0.156	0.043	1.0	205.3	204.3	206.3	0.091	0.065	158.9	28.4	229.5	187.3
η_2	1.427	0.644	117.7	338.3	220.7	96.0	0.524	0.26	71.6	337.6	266	49.2
M_3	0.304	0.006	163.2	18.6	215.4	181.8	0.099	-0.067	90.4	19.6	289.1	110
M_4	0.174	0.040	21.5	68.8	47.3	90.3	0.192	-0.016	140.4	127.2	346.8	267.6
S_4	0.234	0.153	178.5	29.0	210.6	207.5	0.152	0.057	146.8	93.9	307.2	240.7

Table 6

Tidal current analysis results for current meter C4. Results are in tidal ellipse (cm s^{-1}) form. Phases are referred to GMT

	C4S						*C4M*					
NAME	$a^+ + a^-$	$a^+ - a^-$	θ	g	g^+	g^-	$a^+ + a^-$	$a^+ - a^-$	θ	g	g^+	g^-
$2Q_1$	1.524	0.127	85.2	342.7	257.5	67.9	0.864	0.630	61.1	3.3	302.2	64.5
Q_1	2.965	1.891	121.5	190.6	69.1	312.1	1.713	1.269	71.6	231.4	159.8	303.0
O_1	1.727	0.843	67.3	188.4	121.1	255.8	1.638	0.386	138.1	39.4	261.4	177.5
NO_1	1.277	0.049	81.1	280.4	199.3	1.5	1.186	0.364	78.1	306.0	227.9	24.2
P_1	0.881	0.635	71.7	157.5	85.8	229.3	0.866	0.778	101.2	76.9	335.8	178.1
K_1	3.052	1.810	73.9	155.2	81.3	229.1	2.859	2.415	103.3	74.6	331.3	177.9
J_1	0.572	-0.184	117.1	67.6	310.6	184.7	0.611	0.215	150.5	243.0	92.5	33.5
OO_1	3.287	1.327	16.5	295.8	279.3	312.2	1.199	0.336	41.6	34.2	352.7	75.8
ε_2	0.538	0.360	48.3	331.1	282.8	19.4	0.357	0.245	49.6	2.9	313.3	52.6
μ_2	0.471	0.057	74.5	77.2	2.7	151.6	0.507	0.365	47.1	211.4	164.3	258.5
N_2	0.713	0.251	157.7	355.9	198.2	153.6	0.340	0.139	120.6	174.3	53.7	294.9
M_2	0.580	-0.078	130.7	16.9	246.2	147.6	0.552	0.130	162.1	353.8	191.7	155.9
L_2	0.664	-0.024	16.8	355.1	338.4	11.9	0.334	0.164	147.4	308.0	160.6	95.5
S_2	0.378	0.342	160.5	35.5	235.0	196.0	0.410	0.112	18.3	303.7	285.5	322.0
K_2	0.073	0.065	139.5	29.3	249.8	168.8	0.082	0.019	177.3	117.5	300.3	294.8
η_2	1.560	0.355	17.4	131.3	113.9	148.6	1.053	-0.058	117.3	12.7	255.4	129.9
M_3	0.201	-0.132	120.6	343.9	223.3	104.5	0.289	-0.137	142.8	330.0	187.2	112.9
M_4	0.307	0.039	137.0	14.1	237.2	151.1	0.086	0.002	142.2	13.9	231.7	156.0
S_4	0.477	-0.011	132.7	70.3	297.6	203.0	0.164	0.033	162.4	37.9	235.5	200.2

Table 6
Continuation

NAME	$a^+ + a^-$	$a^+ - a^-$	C4B θ	g	g^+	g^-
$2Q_1$	0.353	-0.059	38.4	159.2	120.8	197.6
Q_1	0.865	0.345	48.0	249.1	201.0	297.1
O_1	0.652	0.031	55.7	82.1	26.4	137.8
NO_1	1.182	0.759	63.6	319.8	256.1	23.4
P_1	0.293	0.151	85.9	102.6	16.7	188.5
K_1	1.072	0.354	88.1	100.2	12.2	188.3
J_1	0.403	0.117	147.0	262.1	115.1	49.1
OO_1	0.637	0.469	11.1	30.9	19.8	41.9
ε_2	0.163	-0.147	84.4	108.0	23.6	192.3
μ_2	0.207	-0.018	176.9	34.3	217.4	211.2
N_2	0.187	0.019	154.3	84.7	290.4	238.9
M_2	0.256	0.008	163.3	305.9	142.7	109.2
L_2	0.409	0.124	146.4	280.9	134.5	67.4
S_2	0.224	0.053	144.1	150.9	6.8	295.0
K_2	0.045	0.008	123.1	144.7	21.6	267.8
η_2	0.414	-0.054	174.9	344.1	169.2	159.0
M_3	0.133	0.033	136.2	326.9	190.7	103.1
M_4	0.070	-0.048	175.8	225.7	49.9	41.5
S_4	0.157	-0.085	28.8	79.3	50.5	108.1

Table 7

Comparison between modeled tidal characteristics (Salas-de-León, 1986) and those observed in this paper.

	C1	C2	C3	C4
Amplitude (*cm s^{-1}*)				
Average	0.45	0.30	0.11	0.16
Modeled	0.46	0.32	0.13	0.19
Direction (*degree GMT*)				
This paper	95	108	136	152
Modeled	101	122	125	147

dominant, and modulated the observed tidal current configuration. The semidiurnal components showed low amplitudes at all stations. Sense of rotation of the ellipses varied from north to south. At station 1 the sense of rotation was counterclockwise, while at stations 3 and 4 it was clockwise, in agreement with Salas-de-León (1986) using a depth-integrated numerical model. Present results show a small region of negative rotation southwestward of Arcas Kay, elsewhere in the Bay of Campeche the sense of rotation was positive. The transition was located at station 2 where the upper current meter showed counterclockwise rotation, while the mid-water one showed a clockwise rotation, probably because of the Arcas Kay umbra.

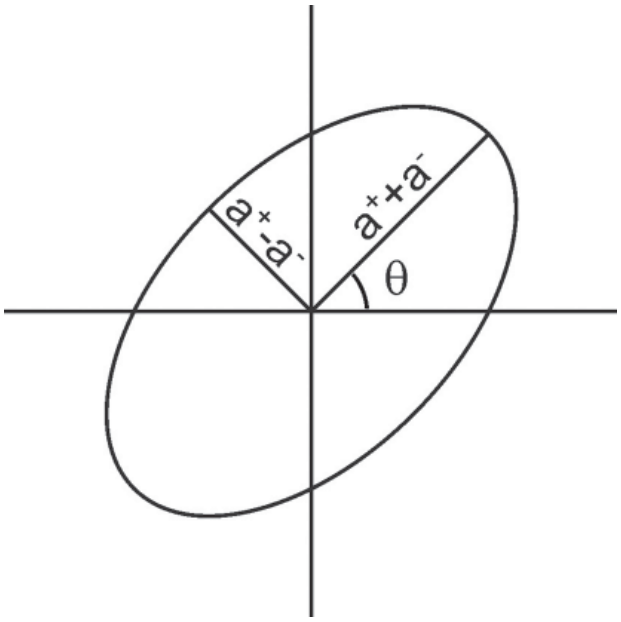

Fig. 3. The tidal ellipse showing major and minor axes, and angle of inclination θ.

The results (Table 7) agree with the modeled amplitudes and directions by Salas-de-León (1986). The modeled amplitudes were slightly higher than those observed, but the difference was less than 15 %. Angles of tidal ellipses as found from the model were higher than observed in the eastern part of the bay (C1, C2). The opposite was true in the western part of the bay (C3, C4). Differences in the angle of the tidal ellipses between those reported in this study and those obtained with the model were less than 11%.

Tidal waves affect currents in different ways with depth as the waves travel at different speeds depending on bathymetry, density differences, and bottom friction. These differences generated vertical phase lag as observed in this study. Amplitude differences from surface to bottom were 0.1 cm s^{-1} at stations 1 and 2 and 0.7 cm s^{-1} at stations 3 and 4. Phase differences from surface to bottom were 30 minutes at stations 1 and 2; 9 minutes at station 3; and 1 h at station 4. The differences in amplitude within the water column are small, but however, the differences in phase at stations 1, 2, and 4 were significant. Near the shelf breaks tidal currents can go up or down, producing a hydraulic jump to compensate for the phase lag by conservation of vorticity. This feature could also modulate the vertical displacement of plankton. Recent observations of vertically

stratified sampling of zooplankton and acoustic Doppler current profilers (ADCP) showed similar patterns in the shelf break of the Bay of Campeche (Monreal-Gómez *et al*., in preparation).

Conclusions

Tidal current analysis in the southern shelf of the Bay of Campeche (Gulf of Mexico) revealed the dominance of constituent K_1 in tidal currents. Differences in amplitude from surface to bottom were negligible but there was a vertical phase lag of up to 1 hour in the south-western-most station. The sense of rotation of the tidal ellipse at station 1, near Arcas Kay, was negative but it was positive at other stations. Arcas Kay had a strong influence on tidal currents, as it's phase and the sense of rotation of the tidal ellipse varied within the water column.

Acknowledgements

This work was supported by PEMEX. We thank INRS-Océanologie, from the University of Québec, Canada, for collaboration in a joint project on coastal circulation in the shelf of the southern Bay of Campeche. This work is a contribution of the Instituto de Ciencias del Mar y Limnología, (ICML) of the Universidad Nacional Autónoma de México (UNAM). Comments on the original manuscript by C. Lomnitz and two anonymous reviewers are greatly appreciated.

Bibliography

EMERY, W. J. and R. E. THOMSON, 1998. Data analysis methods in physical oceanography. Pergamon Press, 634 pp.

GRACE, S. F., 1932. Oceanic tides. *Mon. Not. R. Astron. Soc. Geophys. Suppl. 3*, 70-83.

GODIN, G. G., 1972. The analysis of tides. University of Toronto Press. Toronto, Ontario, Canada, 264 pp.

GODIN, G. G., 1976. The reduction of current observations with the help of the admittance function. Technical note No. 14, Environment Canada, Ottawa, Canada. Marine Environmental Data Service, 13 pp.

FOREMAN, M. G. G., 1996. Manual for tidal currents analysis and prediction. Pacific Marine Science Report 78-6. Institute of Ocean Sciences, Patricia Bay, Victoria, B. C., Canada, 57 pp.

SALAS-DE-LEON, D. A., 1986. Modelisation de la marée M2 et de circulation residuelle dans le Golfe du Mexique, Ph.D. Thesis, 239 pp., Université de Liège, Liège Belgium.

SALAS-DE-LEÓN, D. A. and M. A. MONREAL-GÓMEZ, 1997. Mareas y circulación residual en el Golfo de México. *In:* Monografía No. 3 "Oceanografía Física en México", M.F. Lavín Peregrina, ed. Unión Geofísica Mexicana. México. 201-223 pp.

SALAS-MONREAL, D., 2006. Continously stratified flow dynamics over a hollow. Ph. D. Thesis, Old Dominion University, Norfolk, Virginia, USA, 111 pp.

David Alberto Salas-de-León[1], María Adela Monreal-Gómez[1], David Salas-Monreal[2], Gilberto Expósito-Díaz[1], Mayra Lorena Riverón-Enzastiga[1], Felipe Vázquez-Gutiérrez[1]

[1] *Instituto de Ciencias del Mar y Limnología, Universidad Nacional Autónoma de México, Cd. Universitaria, Del. Coyoacán, 04510 Mexico City, Mexico.*
E-mail: salas@mar.icmy.unam.mx

[2] *Centro de Ecología y Pesquerías, Universidad Veracruzana, Hidalgo 617, Col. Río Jamapa, Boca del Río, 94290 Veracruz, México.*